Follow us @BoneJointRes

Freely available online OPEN ACCESS

BJR

BIOMATERIALS

Human acellular amniotic membrane scaffolds encapsulating juvenile cartilage fragments accelerate the repair of rabbit osteochondral defects

Z. Jun,
W. Yuping,
H. Yanran,
L. Ziming,
L. Yuwan,
Z. Xizhong,
W. Zhilin,
L. Xiaoji

From Zunyi Medical University, Guizhou, China

Aims

The purpose of this study was to explore a simple and effective method of preparing human acellular amniotic membrane (HAAM) scaffolds, and explore the effect of HAAM scaffolds with juvenile cartilage fragments (JCFs) on osteochondral defects.

Methods

HAAM scaffolds were constructed via trypsinization from fresh human amniotic membrane (HAM). The characteristics of the HAAM scaffolds were evaluated by haematoxylin and eosin (H&E) staining, picrosirius red staining, type II collagen immunostaining, Fourier transform infrared spectroscopy (FTIR), and scanning electron microscopy (SEM). Human amniotic mesenchymal stem cells (hAMSCs) were isolated, and stemness was verified by multilineage differentiation. Then, third-generation (P3) hAMSCs were seeded on the HAAM scaffolds, and phalloidin staining and SEM were used to detect the growth of hAMSCs on the HAAM scaffolds. Osteochondral defects (diameter: 3.5 mm; depth: 3 mm) were created in the right patellar grooves of 20 New Zealand White rabbits. The rabbits were randomly divided into four groups: the control group (n = 5), the HAAM scaffolds group (n = 5), the JCFs group (n = 5), and the HAAM + JCFs group (n = 5). Macroscopic and histological assessments of the regenerated tissue were evaluated to validate the treatment results at 12 weeks.

Results

In vitro, the HAAM scaffolds had a network structure and possessed abundant collagen. The HAAM scaffolds had good cytocompatibility, and hAMSCs grew well on the HAAM scaffolds. In vivo, the macroscopic scores of the HAAM + JCFs group were significantly higher than those of the other groups. In addition, histological assessments demonstrated that large amounts of hyaline-like cartilage formed in the osteochondral defects in the HAAM + JCFs group. Integration with surrounding normal cartilage and regeneration of subchondral bone in the HAAM + JCFs group were better than those in the other groups.

Conclusion

HAAM scaffolds combined with JCFs promote the regenerative repair of osteochondral defects.

Cite this article: *Bone Joint Res* 2022;11(6):349–361.

Keywords: HAAM scaffold, JCFs, hAMSCs, Osteochondral defects

Article focus

- How can human acellular amniotic membrane (HAAM) scaffolds be prepared simply and effectively?
- What is the effect of HAAM scaffolds and juvenile cartilage fragments (JCFs) on cartilage regeneration in rabbits?

Key messages

- In vitro, we successfully constructed HAAM scaffolds with a simple, inexpensive method, and confirmed their good cytocompatibility.
- In vivo, we demonstrated that the HAAM scaffolds, combined with JCFs, improved

Correspondence should be sent to Luo Xiaoji; email: cy2982@163.com

doi: 10.1302/2046-3758.116.BJR-2021-0490.R1

Bone Joint Res 2022;11(6):349–361.

effects on cartilage repair, as evidenced by macroscopic and histological evaluation.

Strengths and limitations

- This is the first report to evaluate the effects of HAAM scaffolds and JCFs on the repair of rabbit osteochondral defects.
- Further studies are needed to explore the degradation rates of HAAM scaffolds in vitro and in vivo.

Introduction

Articular cartilage injury is a common problem in orthopaedic clinical practice, frequently occurring in joint trauma. Articular cartilage injury is a significant source of joint pain and has been recognized as one of the contributing factors to significant morbidity and osteoarthritis (OA).[1-6] Self-healing is difficult because of the avascular property and extremely low regeneration of the cartilage tissue.[7] Thus far, many treatments have been attempted to promote cartilage healing, including bone marrow stimulation therapy through microfractures, osteochondral transplantation (autograft or allograft), biomimetic scaffolds, platelet-rich plasma (PRP), and autologous chondrocyte implantation (ACI).[8-17] Although ACI has been identified as the gold standard for the treatment of chondral defects, and has provided good outcomes in prospective randomized trials, there are some inherent limitations, including complicated operating procedures and high treatment costs.[18]

The human amniotic membrane (HAM) is a natural high-molecular-weight biological material that is composed of a basement membrane (BM), an avascular collagenous stroma, a single layer of epithelial cells and underlying fibroblasts.[19] HAM is rich in extracellular matrix (ECM) components, such as fibronectin, laminin, elastin, type I collagen (Col-I), type II collagen (Col-II), and type IV collagen (Col-IV).[20] ECM is a crucial element for tissue reconstruction or organ formation because of its positive effects on the survival, migration, proliferation, and differentiation of cells. In addition, ECM can provide mechanical support and further introduce many biophysical and biochemical stimuli. For instance, ECM in cartilage provides nutrients and mechanical support for chondrocytes.[21] Owing to the unique features and advantages of HAM, it has been widely used in clinical practice and fundamental research. However, there are also some disadvantages associated with fresh HAM, such as the immunogenicity of the tissue, unsuitable preservation methods, and transportation challenges.

Human acellular amniotic membrane (HAAM) scaffolds, which derive from HAM via removal of the cellular components of fresh HAM, have been successfully prepared and applied in tissue regeneration. HAAM scaffolds have some similar properties to fresh HAM, including a network structure, abundant collagen fibres, and an especially ample content of Col-II. Some studies have demonstrated that HAAM could decrease acute liver injury and accelerate tendon-to-bone healing.[22,23] The ECM of articular cartilage is composed of large amounts of aggrecan and collagen, of which Col-II plays an important role in compression resistance. Therefore, HAAM scaffolds with ECM constituents similar to those of articular cartilage may be appropriate materials that can simulate the ECM of articular cartilage and promote cartilage regeneration.

The concept of autologous cartilage fragment implantation was first put forth in 1982, and an animal experiment confirmed the effectiveness of minced cartilage fragment implantation as a cartilage repair procedure in 2006.[24] Since then, this easy and effective procedure has been applied in fundamental research and clinical practice, and good outcomes have been reported. Many studies have demonstrated that autologous cartilage fragments could promote cartilage regeneration.[25-27] Although autologous cartilage fragments have been demonstrated to have a positive effect on cartilage defect repair, there are also some disadvantages of their use, including donor-site complications and limitations in the sizes of the defects.[28,29]

Recently, juvenile cartilage fragments (JCFs) have attracted widespread attention and have been introduced as a new treatment for cartilage repair. The technique requires the preparation of approximately 1 to 2 mm cubes of JCFs from donors and storage at low temperature. The collected JCFs should be used within 45 days to ensure chondrocyte viability.[30,31] To date, many animal studies and clinical studies have demonstrated that JCFs can facilitate the repair of cartilage defects.[32-34] Therefore, JCFs have promising application prospects in cartilage repair.

Although HAAM scaffolds have provided satisfactory outcomes in regenerative medicine, and JCFs have been proven to have good therapeutic effects on cartilage defects, no studies have explored the effect of HAAM scaffolds combined with JCFs on cartilage defects. Therefore, this study aimed to explore whether HAAM scaffolds encapsulating JCFs accelerate the repair of rabbit osteochondral defects. Our hypothesis for this study was that the combined use of HAAM scaffolds and JCFs would facilitate osteochondral repair and cartilage regeneration compared with treatment of defects with HAAM scaffolds or JCFs only.

Methods

hAMSC isolation and culture. A schematic diagram of the experimental procedure is shown in Figure 1. In this experiment, hAMSCs were isolated from the amnions of human placentas in accordance with a previous protocol, and relevant informed consent was provided by each donor before the operation.[35-37] LG-DMEM/F12 medium containing 10% fetal bovine serum (FBS), 1% penicillin/streptomycin, 1% L-glutamine, and 1% non-essential amino acids was used to culture the hAMSCs. The morphology of the hAMSCs was observed under an inverted microscope after three days of cultivation. Third-generation (P3) hAMSCs were used in subsequent

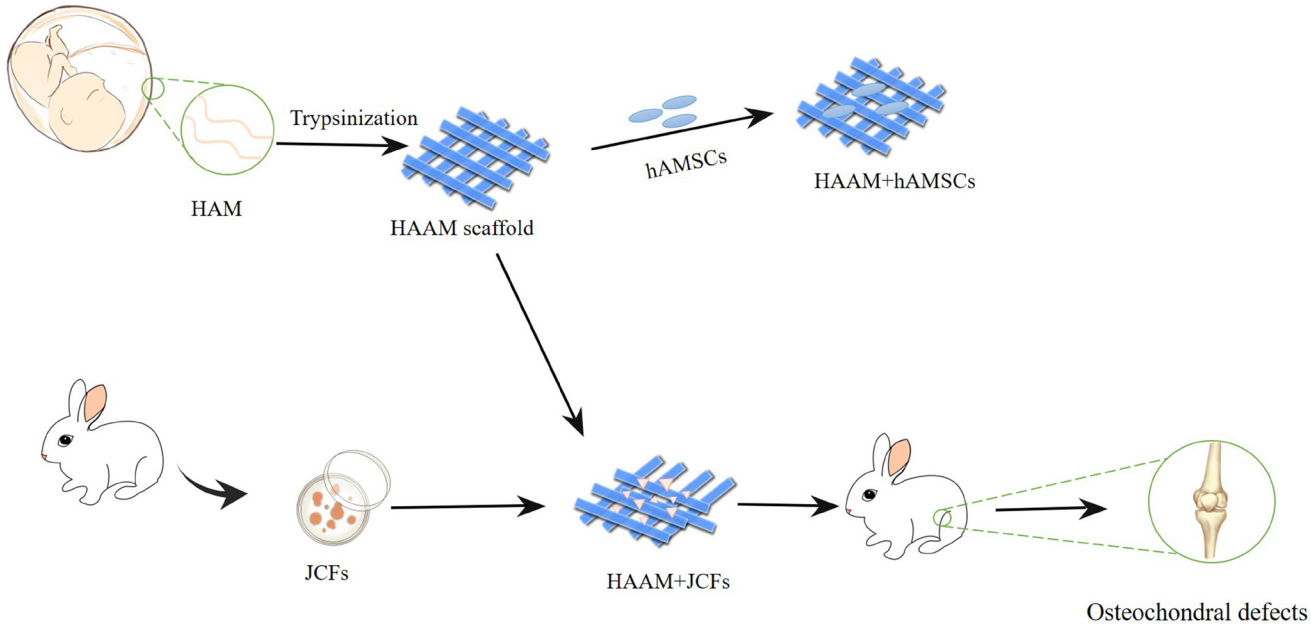

Fig. 1

Schematic diagram of the experimental procedure. HAAM scaffold, human acellular amniotic membrane scaffold; HAM, human amniotic membrane; hAMSCs, human amniotic mesenchymal stem cells; JCFs, juvenile cartilage fragments.

experiments. The stemness of the hAMSCs was tested by osteogenic and chondrogenic differentiation according to previous studies.[35-38] Briefly, hAMSCs were seeded in a six-well plate, and the osteogenic medium (10% FBS, 50 mg/ml ascorbate, 100 nM dexamethasone, and 10 mM β-glycerophosphate) was added when the cell density reached 60%. The results were detected with the BCIP/NBT Alkaline Phosphatase Color Development Kit (Beyotime, China) and alizarin red staining (Solarbio, China). In terms of chondrogenic differentiation, we used Chondrogenic Differentiation Basal Medium (Cyagen, USA) to induce hAMSCs for 14 days; alcian blue staining was used for detection (Solarbio).

Preparation and characterization of HAAM scaffolds. The preparation process of the HAAM scaffolds was conducted as described in a previous article.[13] Briefly, fresh HAM was isolated from the placenta and immediately transferred to the laboratory under low temperature and sterile conditions. The fresh HAM was washed with sterile phosphate-buffered saline (PBS) and cut to approximately 10 × 10 cm. Then, the fresh HAM was carefully placed into a dish with the epithelial layer facing up. The fresh HAM underwent a decellularization process with 0.25% trypsin at 37°C for 30 minutes. Thereafter, a cell scraper was used to remove deciduous epithelial cells from the epithelial layer, and PBS was applied later to thoroughly eliminate debris and epithelial cells. After thorough removal of epithelial cells, we obtained HAAM scaffolds. Then, the HAAM scaffolds were cut to the proper size and placed into six-well culture plates for sterilization. First, the HAAM scaffolds underwent ultraviolet radiation for two hours. Next, they were soaked in a mixture of penicillin, streptomycin, and amphotericin for approximately one hour for further sterilization. After being sterilized by the above-mentioned process, the HAAM scaffolds were ready for use in subsequent experiments. They could attach to the osteochondral defects without glue, or other fixating methods, because of their abundant collagen. The preparation process of the HAAM scaffolds is presented in Figure 2. Haematoxylin and eosin (H&E) staining, picrosirius red staining, type II collagen immunostaining, Fourier transform infrared spectroscopy (FTIR), and scanning electron microscopy (SEM) were used to characterize the HAAM scaffolds. For immunohistochemical staining, a monoclonal mouse anti-rabbit collagen type II antibody (NB600-844; Novus Biologicals, USA) was used. After incubation with a biotinylated secondary anti-mouse antibody (ZSGB-BIO, China), the staining was developed with a 3',3-diaminobenzidine solution (ZSGB-BIO). Then, the sections were counterstained with haematoxylin. Furthermore, to verify removal of cell nuclei and DNA, DNA from fresh HAM and HAAM scaffold were isolated using DNA extraction Kit (D1700, Solarbio) according to the manufacturer instructions. The total DNA from HAM and HAAM scaffold was quantified using a 280 nm UV spectrophotometer.

Seeding hAMSCs on the HAAM scaffolds. After sterilization of the HAAM scaffolds, P3 hAMSCs were seeded on the HAAM scaffolds at a density of 3×10^5 cells/well. LG-DMEM/F12 medium containing 10% FBS, 1% penicillin/streptomycin, 1% L-glutamine, and 1% nonessential amino acids was used to culture the hAMSCs. The morphology and cytoskeletons of the hAMSCs were observed under an inverted phase contrast microscope and stained with phalloidin at days 1, 3, and 7. In addition, the adhesion of

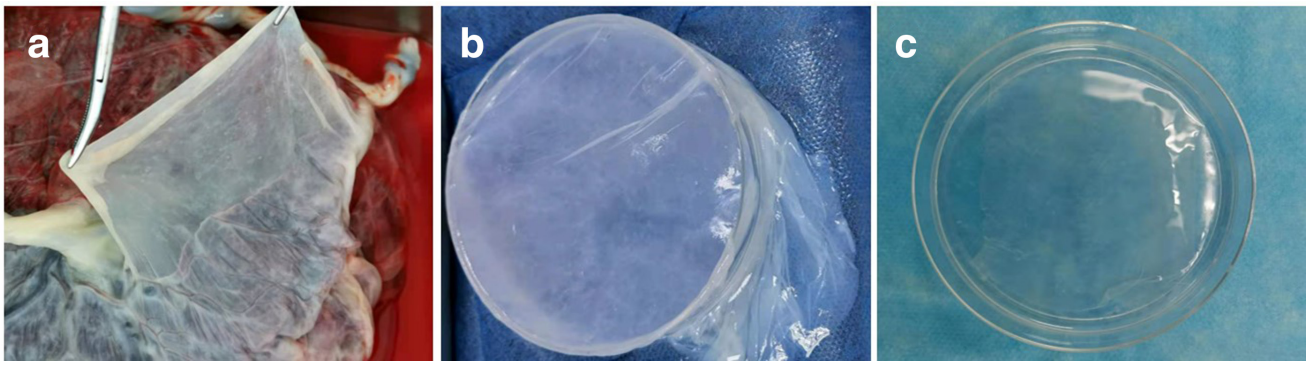

Fig. 2

General preparation process of the human acellular amniotic membrance scaffolds. a) Harvesting of fresh human amniotic membrane (HAM). b) Placement of fresh HAM on a culture dish. c) Decellularization of fresh HAM.

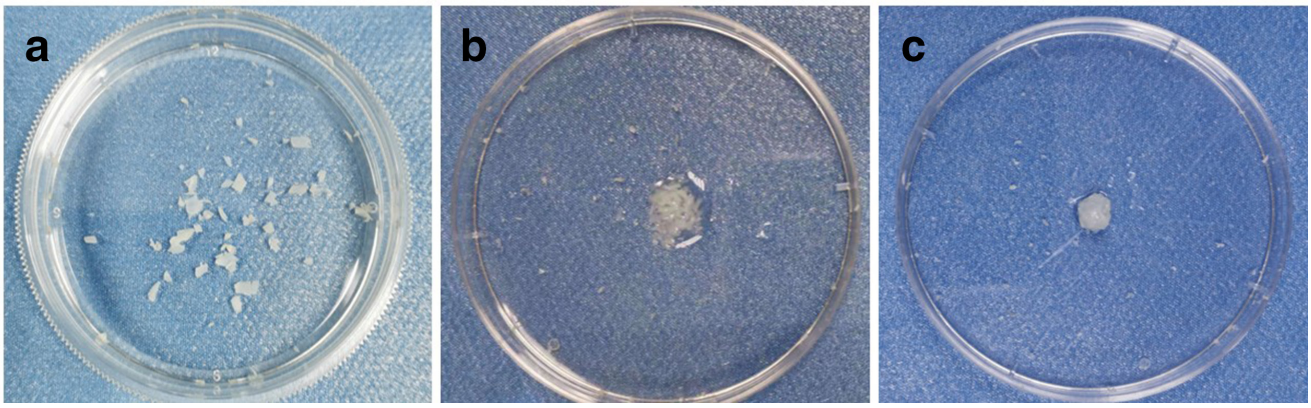

Fig. 3

Preparation of juvenile cartilage fragments (JCFs). a) Harvested juvenile cartilage. b) Harvested juvenile cartilage was cut into JCFs and mixed with saline. c) Moist JCFs were rolled into round shapes.

hAMSCs to the collagenous fibres of the HAAM scaffolds was evaluated by SEM (Hitachi, Japan).

Preparation of juvenile cartilage fragments. On the day of the operation, a total of five juvenile rabbits (two months old) were killed by overdose of 3% sodium pentobarbital to obtain JCFs. The JCFs were prepared for the JCFs group and the HAAM + JCFs group. Briefly, after each rabbit was killed, the bilateral knees were cut under sterile conditions. Then, the articular cartilage was harvested from the articular surface of the distal femur and cut into pieces of approximately 1 mm^3 in size to prepare JCFs with a scalpel. The harvested JCFs were mixed with a small amount of saline to keep them moist and stored aseptically in an aseptic culture dish (Figure 3). To avoid affecting the viability of chondrocytes, the harvested JCFs were kept at 4°C. The harvested JCFs were added to the HAAM scaffolds and wrapped cylindrically with the HAAM scaffolds for use in subsequent experiments. Afterwards, the harvested JCFs and HAAM + JCFs were transplanted into osteochondral defects. An ARRIVE checklist is included in the Supplementary Material to show that the ARRIVE guidelines were adhered to in this study.

Creation of osteochondral defects. Osteochondral defects were created in a total of 20 three-month-old New Zealand rabbits weighing 3.5 to 4.0 kg. The experimental animals were divided into four groups according to the random number method: Group A was the control group, Group B was the HAAM scaffold group, Group C was the JCFs group, and Group D was the HAAM + JCFs group. All procedures were performed as described in a previous article.[34] Briefly, surgery was performed with anaesthesia administered via intramuscular injection of 3% sodium pentobarbital at 0.75 ml/kg. The New Zealand rabbits were placed in the supine position. After shaving, the surgical areas were sterilized with iodine-alcohol. Then, a medial parapatellar incision was made at the right knee joint, and the patella was dislocated laterally to expose the articular surfaces of the trochlear grooves. Osteochondral defects (diameter: 3.5 mm; depth: 3 mm) were created in the centre of the femoral trochlear groove with a dental drill (Figure 4). A total of 20 defects were made in the right knee joints, which were either untreated or treated with HAAM scaffolds, JCFs, and HAAM scaffolds plus JCFs (HAAM + JCFs) (n = 5), and then the incisions

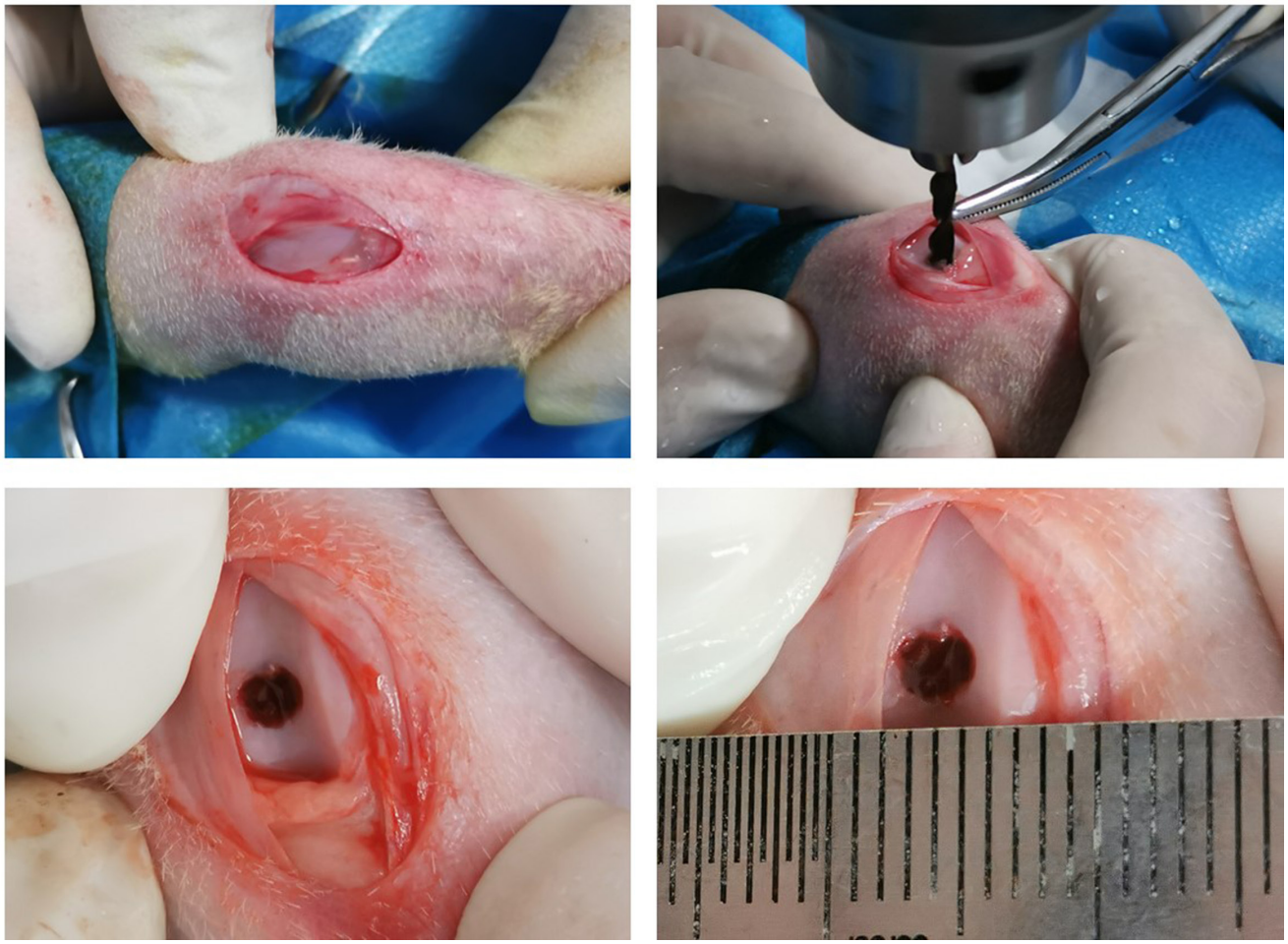

Fig. 4

Procedure for osteochondral defect creation.

were closed layer by layer. Postoperatively, penicillin was injected intramuscularly to prevent infection for three consecutive days. The rabbits were killed at 12 weeks after surgery, and the distal femora were harvested for subsequent tests.

Macroscopic evaluations. After kill, the osteochondral defects were blindly evaluated by three observers (see Acknowledgements) based on the International Cartilage Repair Society (ICRS) evaluation score (Table I) by gross observation.[39] The evaluation was performed from three dimensions: the degree of defect repair, the integration with the border zone, and the macroscopic appearance. The score classification was as follows: one to three points, severely abnormal; four to seven points, abnormal; eight to 11 points, basically normal; and 12 points, completely normal. Macroscopic images of the defects were taken for assessment.

Histological examination. The dissected distal femora were fixed in 4% paraformaldehyde for 24 hours, decalcified for two weeks, and embedded in paraffin for routine histological sectioning. Sagittal sections of approximately 5 μm in thickness were harvested from the centre of each defect and stained with H&E, Safranin O/Fast Green (SO/FG), and toluidine blue (TB), and subjected to IHC staining of Col-II. All samples were scored by the ICRS II evaluation system from the following 14 dimensions: tissue morphological characteristics, matrix staining, cell morphological characteristics, chondrocyte clustering, surface architecture, basal integration, formation of a tidemark, subchondral bone abnormalities, inflammation, abnormal calcification, vascularization, surface assessment, deep zone assessment, and overall assessment.[40]

Statistical analysis. The data are expressed as means and standard deviations (SDs). Statistical analysis (GraphPad Prism 7.0 Software, GraphPad, USA) was performed by one-way analysis of variance (ANOVA) followed by Tukey's multiple comparison test for further evaluation of the differences between the groups unless otherwise stated. $p < 0.05$ was considered to indicate statistical significance.

Results

Culture and characterization of hAMSCs. The morphology of hAMSCs was observed under an inverted phase contrast microscope after three days of cultivation. hAMSCs were adhered to the culture bottle; primary cells showed a spindle-shaped morphology and adherent growth. After

Table I. International Cartilage Repair Society macroscopic evaluation of cartilage repair.

Categories	Score
Degree of defect repair	
In level with surrounding cartilage	4
75% repair of defect depth	3
50% repair of defect depth	2
25% repair of defect depth	1
0% repair of defect depth	0
Integration to border zone	
Complete integration with surrounding cartilage	4
Demarcating border < 1 mm	3
3/4 of graft integrated, 1/4 with a notable border > 1 mm width	2
1/2 of graft integrated with surrounding cartilage, 1/2 with a notable border > 1 mm	1
From no contact to 1/4 of graft integrated with surrounding cartilage	0
Macroscopic appearance	
Intact smooth surface	4
Fibrillated surface	3
Small, scattered fissures of cracks	2
Several, small or few but large fissures	1
Total degeneration of grafted area	0
Overall repair assessment	
Grade I: normal	12
Grade II: nearly normal	11 to 8
Grade III: abnormal	7 to 4
Grade IV: severely abnormal	3 to 1

several subcultures, P3 hAMSCs were obtained and exhibited a uniform vortex-like shape. During the isolation process of hAMSCs, small portions of human amniotic epithelial cells from the amnion were present among the hAMSCs. To reduce the rate of epithelial cells in hAMSCs, we passaged cells and obtained hAMSCs (Figure 5a). To verify the osteogenic differentiation, we examined the ALP activities by ALP staining at day 7. The results indicated that hAMSCs had early osteogenic differentiation activity. Additionally, we performed alizarin red staining to demonstrate the late osteogenic differentiation of hAMSCs at day 21. The results showed that there were calcium deposits, which demonstrated that hAMSCs had late osteogenic differentiation activity. Further, chondrogenic potential was confirmed by alcian blue staining at day 14 (Figure 5b).

Characterization of the HAAM scaffolds. H&E staining showed that epithelial cells were located in the epidermal layer of fresh HAM, and the nuclei of epithelial cells were clearly visible. After treatment by trypsinization, epithelial cells were completely removed, and there were no epithelial cells on the HAAM scaffolds. In addition, the basement membranes of the HAAM scaffolds were intact, and there were no differences between the fresh HAM and HAAM scaffolds (Figure 6a). Furthermore, the picrosirius red staining results showed that there were massive amounts of collagen in both the fresh HAM and HAAM scaffolds (Figure 6b). The chemical properties of the fresh HAM and HAAM scaffolds were identified by FTIR (Figure 7). The results showed that no new chemical bonds appeared in the HAAM scaffolds, suggesting that the HAAM scaffolds had chemical properties similar to those of fresh HAM. IHC staining demonstrated Col-II positivity in both fresh HAM and HAAM scaffolds (Figure 6c). The SEM results showed that fresh HAM and HAAM scaffolds had abundant collagen structures and networks of spatial structure. Although fresh HAM was treated by trypsinization, the collagen structure was not destroyed. A large amount of collagen constituted a network, which was beneficial to cell growth (Figure 6d).

Seeding hAMSCs on the HAAM scaffolds. After one, three, and seven days of cultivation, the adhesion and proliferation of hAMSCs on the HAAM scaffolds were evaluated. On day 1, we observed a few hAMSCs on the surfaces of the HAAM scaffolds. After continuous culture, the numbers of hAMSCs gradually increased. On day 7, the surfaces of the HAAM scaffolds were almost completely coated with hAMSCs (Figure 8a). The cytoskeletons of hAMSCs on the surfaces of the HAAM scaffolds were labelled with phalloidin and 6-diamidino-2-phenylindole dilactate (DAPI), which stained the f-actin protein red and the nuclei blue. The results showed that cells on the HAAM scaffold surfaces spread well and had normal cytoskeletal arrangements (Figure 8b). SEM showed hAMSCs adhered to collagenous fibres of the HAAM scaffolds (Figure 8c). Cells gradually increased in number and adhered to the HAAM scaffolds, which demonstrated that the HAAM scaffolds did not inhibit cell adhesion or proliferation. This was mainly attributed to the high porosity, large surface area, and well-interconnected pore network structure. Taken together, the data indicated that the HAAM scaffolds had excellent cytocompatibility and did not affect cell adhesion or proliferation.

Macroscopic observations. During the whole observation period, no deaths occurred in any group. No wound or joint infection was observed in any of the joints, and all samples were followed. At 12 weeks after surgery, the gross morphological observations showed that the osteochondral defects in the HAAM + JCFs group were completely covered with newly regenerated tissue and had a smooth surface that was similar to that of native cartilage. In addition, the colour and lustre of the regenerated tissue were similar to those of native cartilage. The boundary between the regenerated tissue and native cartilage had almost completely disappeared. In the JCFs group and the HAAM group, we observed partially filled osteochondral defects in newly repaired tissue that had nonuniform and irregular surfaces compared with those of native cartilage. The margins between the native cartilage and new cartilage were partially identified. In the control group, although small amounts of newly formed tissue were observed in osteochondral defects, the colour and surfaces were distinctly different from those of normal cartilage. The boundary could be easily identified (Figure 9a). The ICRS macroscopic scores were apparently higher in the HAAM + JCFs group than in the other three groups. The score of the control group was

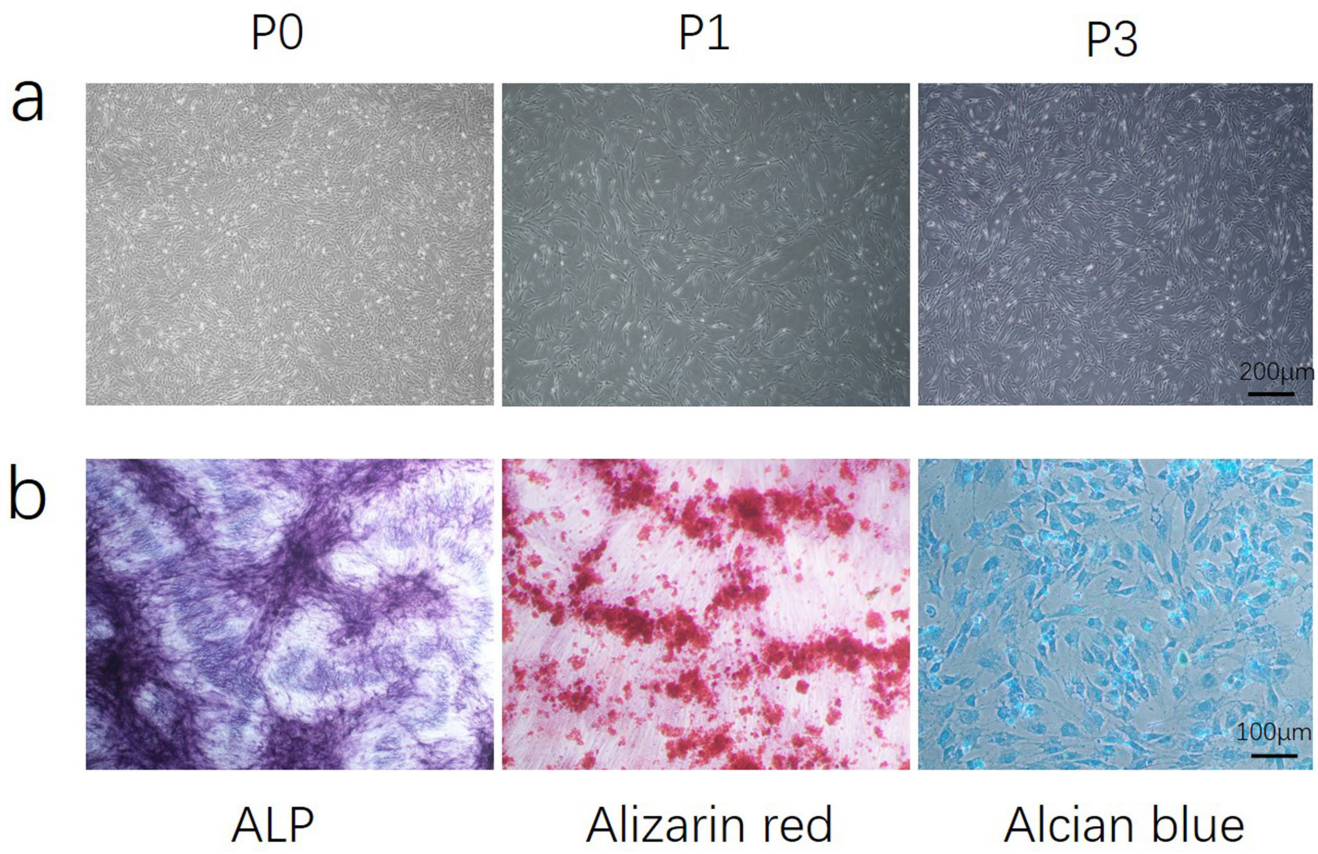

Fig. 5

a) Microscopic observations of passage-0 to passage-3 human amniotic mesenchymal stem cells (hAMSCs). Scale bar: 200 μm. b) Multiple differentiation potential (for osteogenic and chondrogenic differentiation) of passage-3 hAMSCs. Osteogenic differentiation potential was detected by alkaline phosphatase (ALP) staining and alizarin red staining; chondrogenic differentiation potential was detected by Alcian blue staining. Scale bar: 100 μm.

lower than those of the other three groups. There was a difference between the JCFs group and the HAAM group (Figure 9b).

Histological assessment. Histological staining assessment further confirmed that, compared to the HAAM group, JCFs group, and the control group, HAAM + JCFs facilitated the repair of rabbit articular cartilage and subchondral bone. At 12 weeks, the defect centre of the control group remained vacant, and the boundary between the regenerative and adjacent normal cartilage could be identified easily. There was almost no newly formed cartilage in the defect areas, and only some irregular soft-tissues filled the osteochondral defects. The reparative soft-tissues were negative for SO/FG and TB staining, suggesting that no glycosaminoglycans (GAGs) were formed in the control group. Furthermore, IHC staining of Col-II also presented negative results in the control group. In the JCFs group, we observed newly regenerative tissues filling the whole osteochondral defects, and some cartilage fragments in the defects were distinguished. The thickness and tissue continuity of the regenerative tissues were worse than those of the cartilage in the HAAM group, the cartilage in the HAAM + JCFs group and native cartilage. As observed by SO/FG staining and TB staining, GAGs were less abundant in the JCFs group than in the HAAM group, the HAAM + JCFs group, and native cartilage. The IHC staining results were weakly positive, indicating little Col-II formation. In the HAAM group, cartilage repair was obvious, and the osteochondral defects were fully filled with regenerative tissues. The newly formed cartilaginous ECM was detected by SO/FG, TB, and IHC staining of Col-II, and the results were strongly positive. However, the continuity and smoothness of the newly formed cartilage were inferior to those of the normal cartilage. In the HAAM + JCFs group, we not only observed newly formed cartilage filling in the defects, but also found smooth and continuous cartilage that was similar to native cartilage. The results of SO/FG, TB, and IHC staining of Col-II were all superior to those in the other three groups, and new regenerative subchondral bone was observed (Figure 10). At 12 weeks after surgery, the scores in any of the subclass scores of HAAM + JCFs were better than those in other groups, with statistical differences ($p < 0.05$, one-way ANOVA).

Discussion

This study demonstrates the feasibility of repairing osteochondral defects with HAAM scaffolds encapsulating

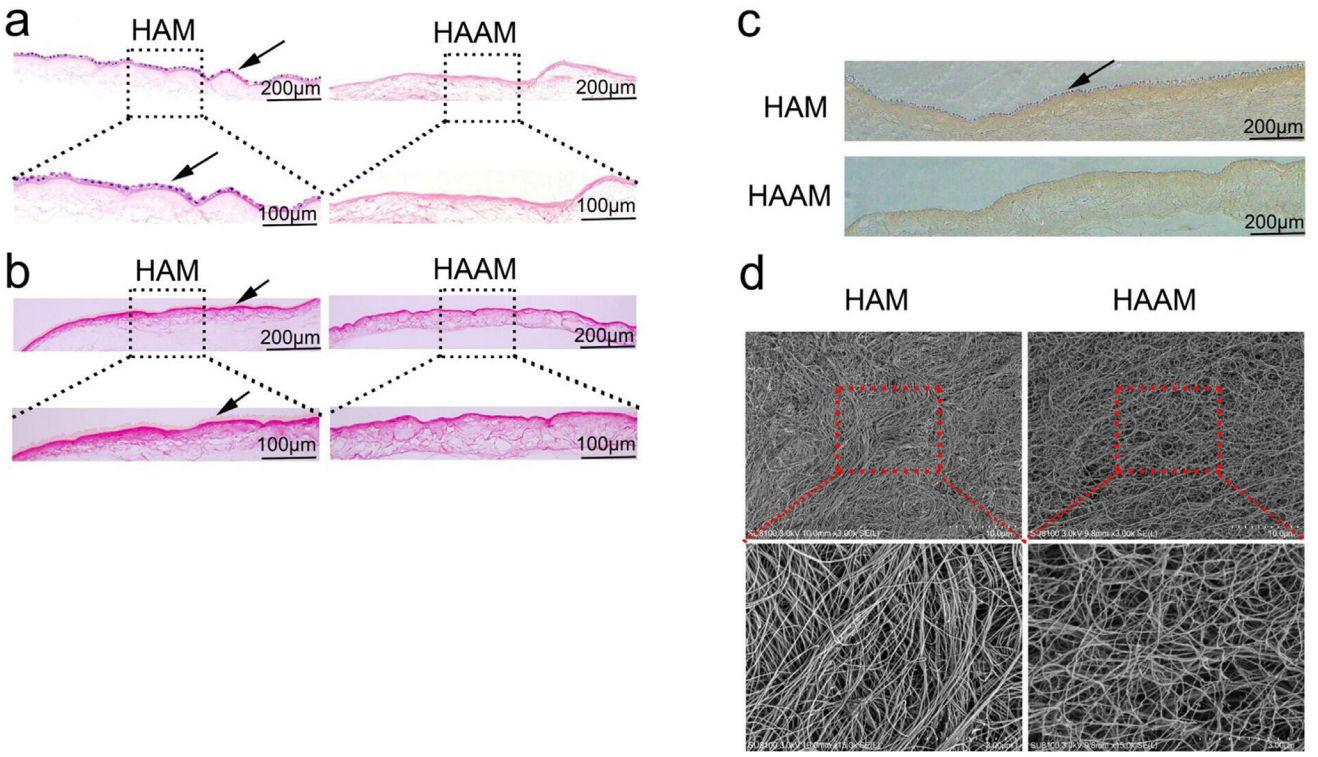

Fig. 6

Characterization of the human acellular amniotic membrane (HAAM) scaffolds. a) Haematoxylin and eosin staining. b) Picrosirius red staining. c) Immunohistochemical staining of collagen II. d) Scanning electron microscope observation. The black arrows indicate the epithelial cells on fresh human amniotic membrane (HAM).

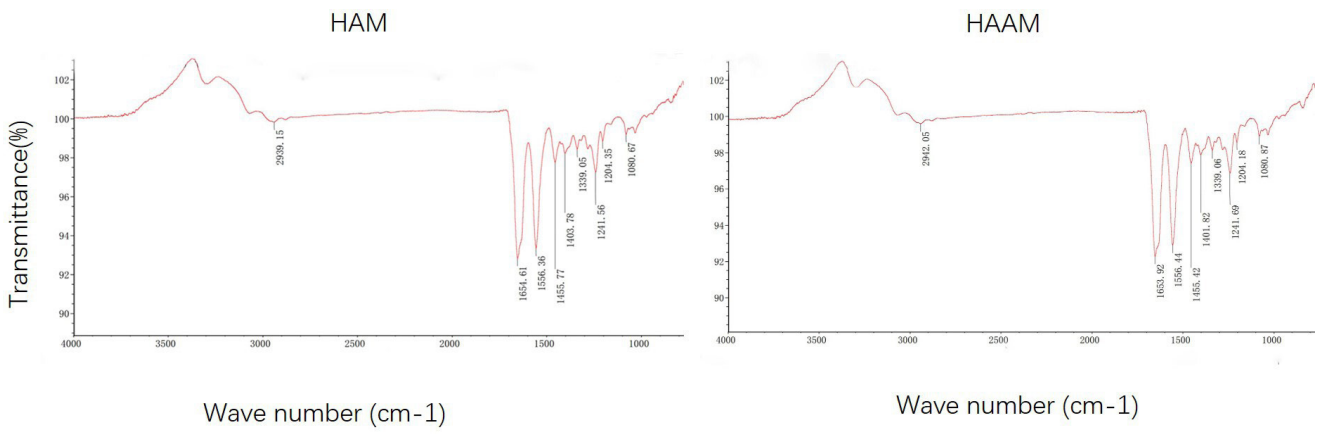

Fig. 7

Fourier transform infrared spectroscopy for human amniotic membrane (HAM) and human acellular amniotic membrane scaffolds (HAAM).

JCFs. In vitro, we successfully constructed HAAM scaffolds with a simple, inexpensive method, and confirmed their good cytocompatibility. In vivo, we demonstrated that the HAAM scaffolds combined with JCFs had improved effects on cartilage repair, as evidenced by macroscopic and histological evaluation. Although the potential mechanisms of this treatment are not clear, the HAAM scaffolds played important roles in osteochondral repair and cartilage regeneration.

HAAM scaffolds are natural biological materials and have the following advantages compared with other biological scaffolds or synthetic scaffolds: first, the scaffolds have widespread sources and carry no ethical or moral controversies; the HAAM scaffolds were prepared from fresh HAM from discarded placentas. Second, the preparation process of HAAM scaffolds is simple and inexpensive relative to the preparation techniques for other scaffolds, such as electrostatic spinning, 3D printing, and

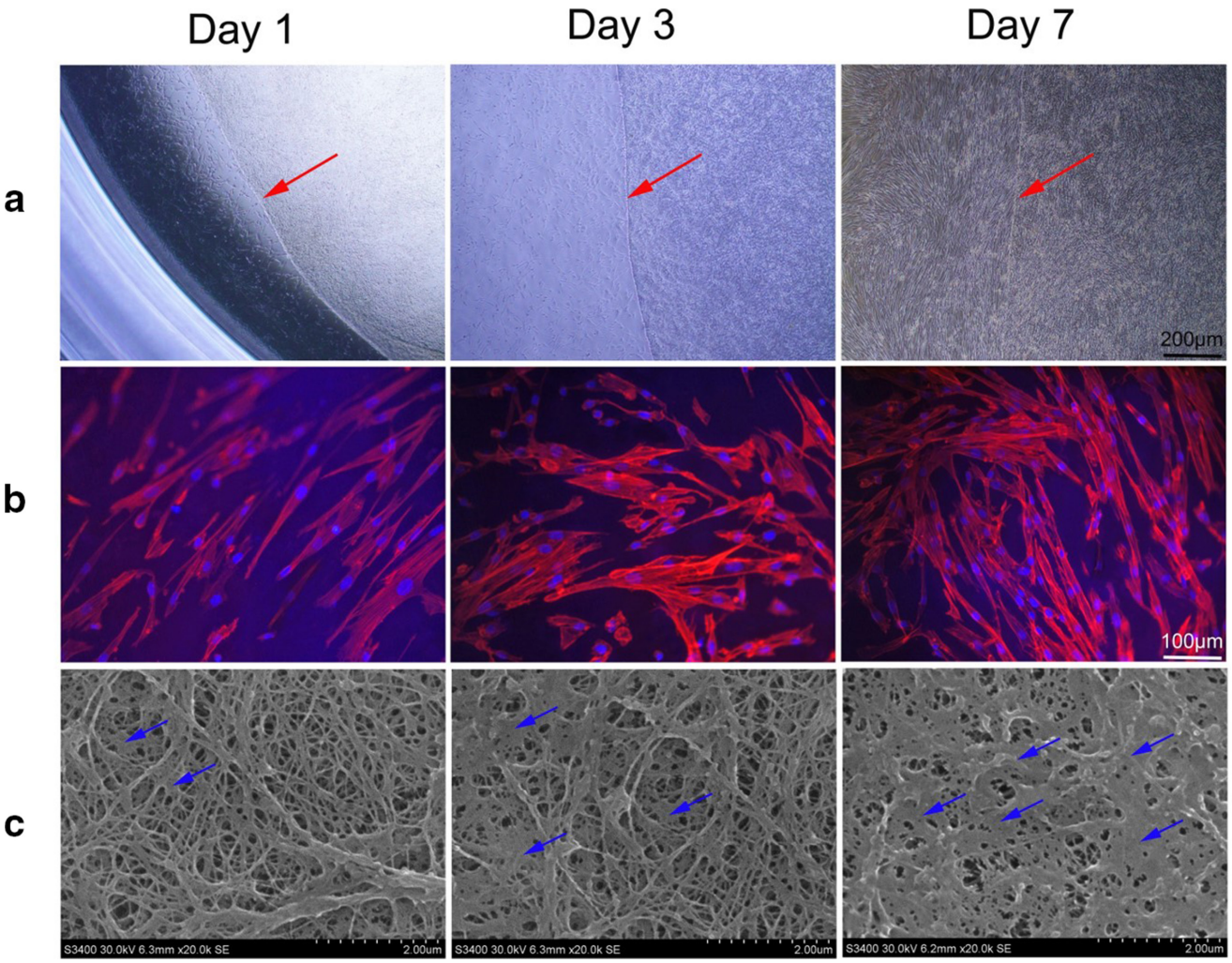

Fig. 8

Human amniotic mesenchymal stem cells (hAMSCs) on human acellular amniotic membrane (HAAM) scaffolds. a) Microscopic observation of hAMSCs on a HAAM scaffold. The red arrows indicate the junction of the HAAM scaffold and the cultureware. The left side of the red arrows is the bottom of the cultureware, and the right side is the HAAM scaffold. Scale bar: 200 μm. b) Cytoskeletal staining of hAMSCs cocultured with a HAAM scaffold. Scale bar: 100 μm. c) Typical scanning electron microscope images of hAMSCs on a HAAM scaffold. The blue arrows indicate hAMSCs. Scale bar: 2 μm.

melt electrowriting (MEW). Moreover, the HAAM scaffolds possess favourable biocompatibility, and no immunological rejection occurs after they are implanted in vivo. We eliminated the immunogenicity of fresh HAM by denuding the epithelial cells, but without destroying its original collagen fibre arrangement and ECM structure, making the resulting scaffolds suitable for cell adhesion/proliferation and in vivo transplantation.

In this study, we prepared HAAM scaffolds by trypsinization to remove epithelial cells. However, we did not eliminate the hAMSCs of fresh HAM because hAMSCs express low levels of costimulatory molecules (CD80, CD83, and CD86) and major histocompatibility type I antigens (human leucocyte antigen (HLA)-A, HLA-B, and HLA-C),[41] suggesting that hAMSCs have low immunogenicity and do not provoke immunological rejection in the host after transplantation. Moreover, hAMSCs have been proven to have the capacity to facilitate cartilage regeneration in a previous study.[34] H&E staining demonstrated that the epithelial cells in the epidermal layer of fresh HAM were removed completely and that the HAAM scaffolds maintained the integrated ECM structure. Further detection confirmed that the HAAM scaffolds contained large amounts of collagen fibres and possessed a fibrous reticular structure. The abundant collagen fibres signified sufficient mechanical strength, and the porous structure provided enough space for cell adhesion and proliferation. To test the cytocompatibility, we seeded P3 hAMSCs on the HAAM scaffolds and observed the fates of these cells. Phalloidin staining and SEM demonstrated that hAMSCs could survive and proliferate on the HAAM scaffolds. After seven days of cultivation, hAMSCs fused to patches and almost covered the whole surfaces of the HAAM scaffolds. In addition, the spatial structures of

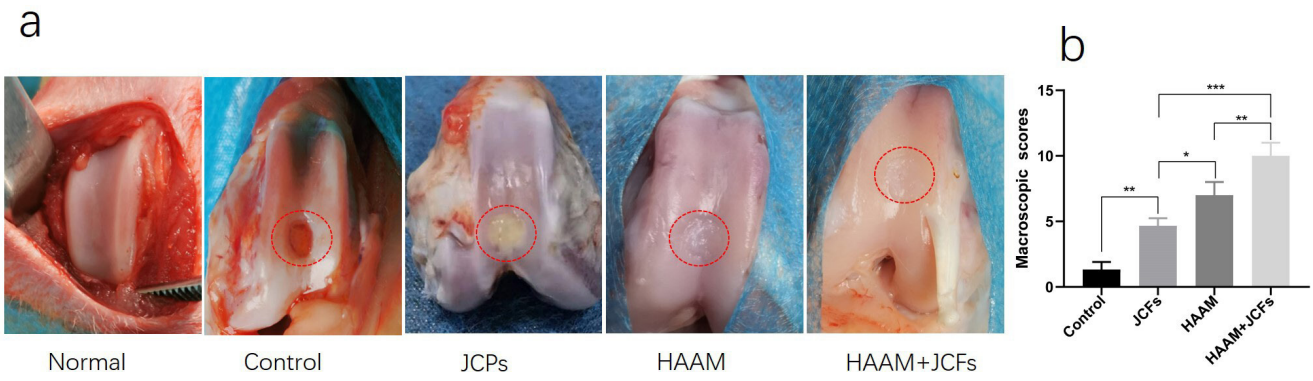

Fig. 9

Macroscopic observations of regenerative tissue at 12 weeks. a) Regenerated tissue of all groups. b) Mean International Cartilage Repair Society macroscopic scores of groups at 12 weeks after surgery (n = 5). *p < 0.05; **p < 0.01; ***p < 0.001. HAAM, human acellular amniotic membrane; JCFs, juvenile cartilage fragments.

the HAAM scaffolds did not change the growth pattern or morphology of hAMSCs. Different types of cells were cultured on HAAM scaffolds to explore the effect of HAAM scaffolds on cells, and to further confirm their capacity for tissue repair. Sanluis-Verdes et al[42] cultured epidermal stem cells and fibroblasts on opposite sides of HAAM scaffolds to fabricate a skin substitute with both epidermal and dermal structures. Zhou et al[43] seeded induced pluripotent stem cell-derived epithelial stem cells on HAAM scaffolds to prepare a skin substitute and evaluated the effects on wound repair. In another study, Wu et al[44] used adipose-derived stem cells as seed cells and cultured them on HAAM scaffolds to repair skin defects. Nevertheless, there have been no reports of hAMSCs cultured on HAAM scaffolds. Compared with other MSC sources,[45-48] hAMSCs have many advantages. Their convenient and non-invasive collection methods, lack of ethical controversies, and high viability and multilineage differentiation ability have led to extensive application of hAMSCs in the treatment of bone and spinal traumas, and in vascular reconstruction surgery.[49-52] In addition, both the cells (hAMSCs) and scaffolds (HAAM scaffolds) come from the placenta, which is more convenient than other tissues for isolation of cells and preparation of scaffolds. Therefore, we cultured hAMSCs on HAAM scaffolds to explore the cytocompatibility of HAAM scaffolds in this study.

JCFs provide a new allograft method for the treatment of osteochondral defects. Although ACI has been regarded as the gold standard for the treatment of chondral defects and has the ability to yield hyaline-like tissues that are more similar to native cartilage at the mechanical, histological, and clinical levels than those formed by other treatments, it requires multistep surgical procedures and a time-consuming process of chondrocyte expansion in vitro.[53] Sufficient chondrocytes are obtained only by monolayer expansion of autologous cells in autologous chondrocyte implantation, which may increase the underlying risk of chondrocyte dedifferentiation.[54] Therefore, cartilage fragment implantation (via autograft or allograft) has been developed to overcome these limitations. Furthermore, the researcher also used autologous meniscus fragments to enhance meniscus repair.[55] Compared to autologous cartilage fragment implantation, allogenic cartilage fragment implantation can overcome the disadvantages of donor site complications and limitations in the sizes of defects that are eligible for repair. Therefore, many animal studies and clinical studies have explored the effects of allogenic cartilage fragments on cartilage repair. To date, mounting evidence has demonstrated that JCFs may be a better choice for cartilage repair than adult cartilage fragments because of their unique advantages. Many studies have reported that adult cartilage fragments have an age-dependent decline in chondrogenic potential.[56,57] In addition, chondrocytes from JCFs are more efficient at actively migrating than those from adult cartilage fragments because they disintegrate the local ECM network at their migrating front.[5] Additionally, a report has indicated that chondrocytes from JCFs express the cell-surface proteins chondromodulin I, B7-H1, and B7-DC, which can suppress immune cell proliferation.[58] In the present study, two-month-old New Zealand White rabbits were used to harvest JCFs. Then, the JCFs were implanted into osteochondral defects alone or with the HAAM scaffolds to promote osteochondral repair.

In vivo, macroscopic and histological assessments demonstrated that the HAAM + JCFs group had a better cartilage repair effect than the other groups. The following possible reasons may explain the above results. First, the HAAM scaffolds provided a suitable microenvironment for endogenous cell migration and growth, especially for bone marrow mesenchymal stem cells (BMSCs) located under subchondral bone and chondrocytes migrating from JCFs, which play a key role in cartilage repair. Second, juvenile chondrocytes produced by the JCFs facilitated regeneration of cartilage because of their chondrogenic potential to generate hyaline-like neocartilage. Therefore, the good outcomes were ultimately attributable to the synergetic effects of the HAAM scaffolds

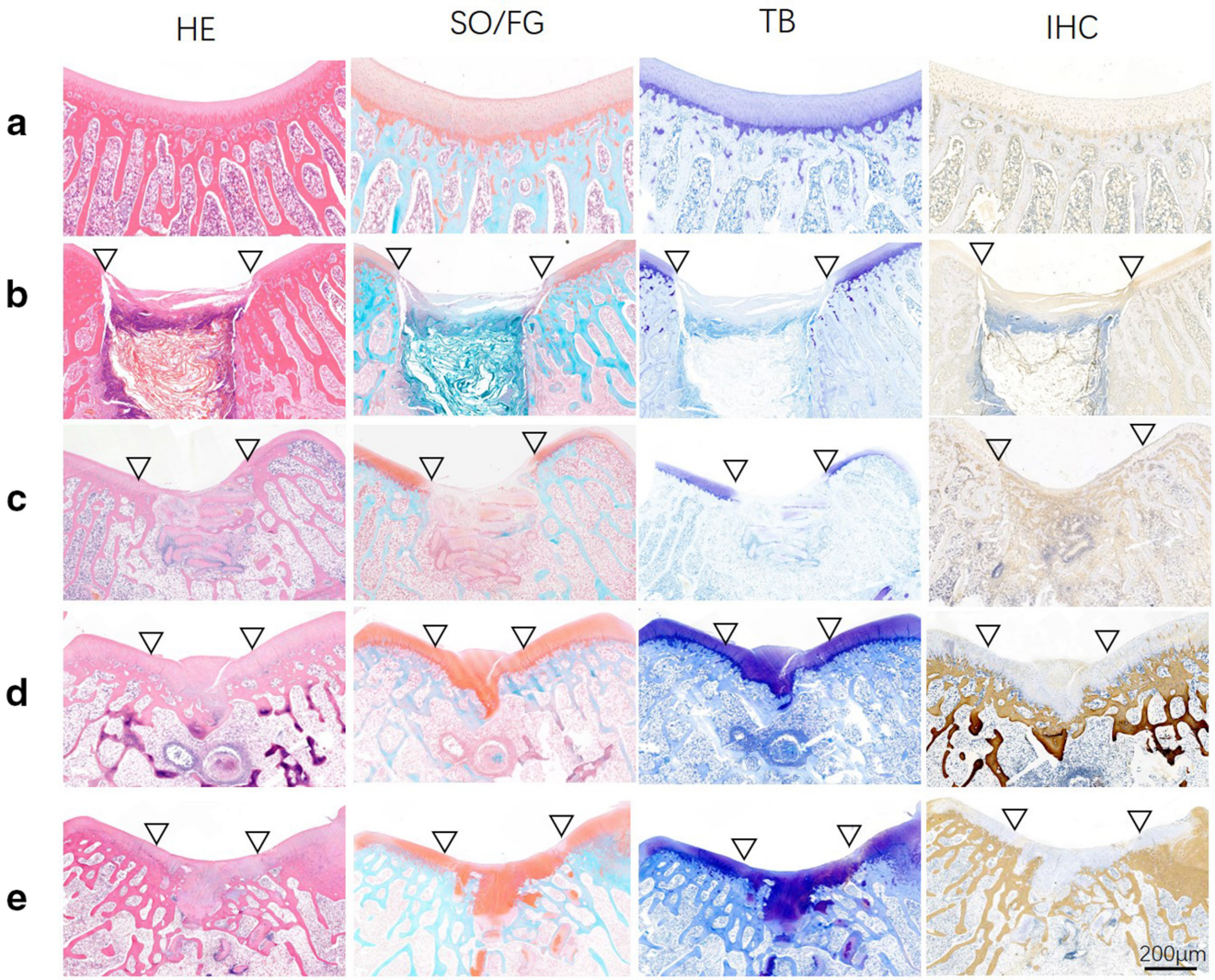

Fig. 10

Histological assessment of regenerated tissue in all groups at 12 weeks after surgery (n = 5). ∇: boundary of defects. a) Normal group. b) Control group. c) Juvenile cartilage fragments (JCFs) group. d) Human acellular amniotic membrane (HAAM) group. e) HAAM + JCFs group. HE, haematoxylin and eosin; IHC, immunohistochemical staining; SO/FG, Safranin O/Fast Green staining; TB, toluidine blue staining of type II collagen. Scale bar: 200 μm.

and JCFs. However, it was surprising that the results of the JCFs group were not as good as we expected, and were inferior to previous experimental outcomes.[33,34,59] The foremost reason was that we did not use fibrin glue to immobilize JCFs at the defects, which might have resulted in JCF loss when bleeding occurred or the knee joint moved. In addition, the JCFs may have been heterogeneous in size and not cut into small enough pieces, hindering effective migration of chondrocytes from JCFs. Therefore, in subsequent experiments, we will resolve these two possible limitations of this study and further confirm the effect of JCFs on cartilage regeneration.

This study also had some limitations. First, we did not detect the degradation of the HAAM scaffolds in vivo. Further studies are needed to explore the degradation rates of HAAM scaffolds in vitro and in vivo, which will provide convincing evidence for other fundamental studies and clinical applications. Second, we did not track the transplanted JCFs or the migration of chondrocytes from JCFs. Therefore, it is difficult to explain the specific effects and mechanism of transplanted JCFs on cartilage regeneration. In addition, only one timepoint (12 weeks) was set to assess cartilage repair in this study, although some other researchers have also chosen only one timepoint to explore cartilage repair.[7,60] Cartilage healing is a gradually developing process, so different timepoints should be chosen to explore the healing process in further studies. Last, we did not coculture the HAAM scaffolds and JCFs in vitro. In vitro, we seeded hAMSCs on HAAM scaffold just to detect the cytocompatibility of the scaffold with cells. Therefore, the chemotactic effect of the HAAM scaffolds on chondrocytes produced by JCFs is still undefined.

In conclusion, this study has demonstrated that HAAM scaffolds encapsulating JCFs have the potential to repair osteochondral defects. We successfully constructed HAAM scaffolds with a simple, low-cost, and effective method. In addition, we demonstrated that the HAAM scaffolds had good cytocompatibility and that the hAMSCs grew well on the HAAM scaffolds. Because of the excellent cytocompatibility, and a similar ECM to that of articular cartilage, HAAM scaffolds may be promising biological scaffolds for cartilage regeneration. Further, JCFs may be a promising method for the treatment of osteochondral defects that will be widely used in clinic.

Supplementary material

ARRIVE checklist.

References

1. **Hunter W**. Of the structure and disease of articulating cartilages. *Clin Orthop Relat Res*. 1995;42(317):3–6.
2. **Nelson AE**, **Allen KD**, **Golightly YM**, **Goode AP**, **Jordan JM**. A systematic review of recommendations and guidelines for the management of osteoarthritis: The chronic osteoarthritis management initiative of the U.S. bone and joint initiative. *Semin Arthritis Rheum*. 2014;43(6):701–712.
3. **Duan M**, **Wang Q**, **Liu Y**, **Xie J**. The role of TGF-*β2* in cartilage development and diseases. *Bone Joint Res*. 2021;10(8):474–487.
4. **Wang X**, **Wang D**, **Xia P**, **et al**. Ultrasound-targeted simvastatin-loaded microbubble destruction promotes OA cartilage repair by modulating the cholesterol efflux pathway mediated by PPARγ in rabbits. *Bone Joint Res*. 2021;10(10):693–703.
5. **Zhang H**, **Li J**, **Xiang X**, **et al**. Tert-butylhydroquinone attenuates osteoarthritis by protecting chondrocytes and inhibiting macrophage polarization. *Bone Joint Res*. 2021;10(11):704–713.
6. **Im GI**. Current status of regenerative medicine in osteoarthritis: stem cells, exosomes, and genes. *Bone Joint Res*. 2021;10(2):134–136.
7. **Wong C-C**, **Chen C-H**, **Chan WP**, **et al**. Single-stage cartilage repair using platelet-rich fibrin scaffolds with autologous cartilaginous grafts. *Am J Sports Med*. 2017;45(13):3128–3142.
8. **Albright JC**, **Daoud AK**. Microfracture and Microfracture Plus. *Clin Sports Med*. 2017;36(3):501–507.
9. **Lu Y**, **Dhanaraj S**, **Wang Z**, **et al**. Minced cartilage without cell culture serves as an effective intraoperative cell source for cartilage repair. *J Orthop Res*. 2006;24(6):1261–1270.
10. **Peterson L**, **Vasiliadis HS**, **Brittberg M**, **Lindahl A**. Autologous chondrocyte implantation: a long-term follow-up. *Am J Sports Med*. 2010;38(6):1117–1124.
11. **Qiao Z**, **Lian M**, **Han Y**, **et al**. Bioinspired stratified electrowritten fiber-reinforced hydrogel constructs with layer-specific induction capacity for functional osteochondral regeneration. *Biomaterials*. 2021;266:120385.
12. **Yanke AB**, **Tilton AK**, **Wetters NG**, **Merkow DB**, **Cole BJ**. DeNovo NT particulated juvenile cartilage implant. *Sports Med Arthrosc Rev*. 2015;23(3):125–129.
13. **Slimi F**, **Zribi W**, **Trigui M**, **et al**. The effectiveness of platelet-rich plasma gel on full-thickness cartilage defect repair in a rabbit model. *Bone Joint Res*. 2021;10(3):192–202.
14. **Rajagopal K**, **Ramesh S**, **Walter NM**, **Arora A**, **Katti DS**, **Madhuri V**. In vivo cartilage regeneration in a multi-layered articular cartilage architecture mimicking scaffold. *Bone Joint Res*. 2020;9(9):601–612.
15. **Tamaddon M**, **Blunn G**, **Xu W**, **et al**. Sheep condyle model evaluation of bone marrow cell concentrate combined with a scaffold for repair of large osteochondral defects. *Bone Joint Res*. 2021;10(10):677–689.
16. **Chen C-H**, **Kang L**, **Chang L-H**, **et al**. Intra-articular low-dose parathyroid hormone (1-34) improves mobility and articular cartilage quality in a preclinical age-related knee osteoarthritis model. *Bone Joint Res*. 2021;10(8):514–525.
17. **Binder H**, **Hoffman L**, **Zak L**, **Tiefenboeck T**, **Aldrian S**, **Albrecht C**. Clinical evaluation after matrix-associated autologous chondrocyte transplantation: a comparison of four different graft types. *Bone Joint Res*. 2021;10(7):370–379.
18. **Niethammer TR**, **Pietschmann MF**, **Horng A**, **et al**. Graft hypertrophy of matrix-based autologous chondrocyte implantation: a two-year follow-up study of NOVOCART 3D implantation in the knee. *Knee Surg Sports Traumatol Arthrosc*. 2014;22(6):1329–1336.
19. **Bourne GL**. The microscopic anatomy of the human amnion and chorion. *Am J Obstet Gynecol*. 1960;79(6):1070–1073.
20. **Wilshaw S-P**, **Kearney JN**, **Fisher J**, **Ingham E**. Production of an acellular amniotic membrane matrix for use in tissue engineering. *Tissue Eng*. 2006;12(8):2117–2129.
21. **Mobasheri A**, **Rayman MP**, **Gualillo O**, **Sellam J**, **van der Kraan P**, **Fearon U**. The role of metabolism in the pathogenesis of osteoarthritis. *Nat Rev Rheumatol*. 2017;13(5):302–311.
22. **Yuan J**, **Li W**, **Huang J**, **et al**. Transplantation of human adipose stem cell-derived hepatocyte-like cells with restricted localization to liver using acellular amniotic membrane. *Stem Cell Res Ther*. 2015;6:217.
23. **Zhang J**, **Liu Z**, **Li Y**, **et al**. FGF-2-Induced Human Amniotic Mesenchymal Stem Cells Seeded on a Human Acellular Amniotic Membrane Scaffold Accelerated Tendon-to-Bone Healing in a Rabbit Extra-Articular Model. *Stem Cells Int*. 2020;2020:4701476.
24. **Albrecht F**, **Roessner A**, **Zimmermann E**. Closure of osteochondral lesions using chondral fragments and fibrin adhesive. *Arch Orthop Trauma Surg*. 1983;101(3):213–217.
25. **Cole BJ**, **Farr J**, **Winalski CS**, **et al**. Outcomes after a single-stage procedure for cell-based cartilage repair: a prospective clinical safety trial with 2-year follow-up. *Am J Sports Med*. 2011;39(6):1170–1179.
26. **Christensen BB**, **Foldager CB**, **Jensen J**, **Lind M**. Autologous dual-tissue transplantation for osteochondral repair: early clinical and radiological results. *Cartilage*. 2015;6(3):166–173.
27. **Christensen BB**, **Foldager CB**, **Olesen ML**, **Hede KC**, **Lind M**. Implantation of autologous cartilage chips improves cartilage repair tissue quality in osteochondral defects: a study in Göttingen minipigs. *Am J Sports Med*. 2016;44(6):1597–1604.
28. **Giza E**, **Delman C**, **Coetzee JC**, **Schon LC**. Arthroscopic treatment of talus osteochondral lesions with particulated juvenile allograft cartilage. *Foot Ankle Int*. 2014;35(10):1087–1094.
29. **Hunziker EB**, **Lippuner K**, **Keel MJB**, **Shintani N**. An educational review of cartilage repair: precepts & practice--myths & misconceptions--progress & prospects. *Osteoarthr Cartil*. 2015;23(3):334–350.
30. **Grawe B**, **Burge A**, **Nguyen J**, **et al**. Cartilage regeneration in full-thickness patellar chondral defects treated with particulated juvenile articular allograft cartilage: an MRI analysis. *Cartilage*. 2017;8(4):374–383.
31. **Tompkins M**, **Adkisson HD**, **Bonner KF**. DeNovo NT allograft. *Oper Tech Sports Med*. 2013;21(2):82–89.
32. **Ao Y**, **Li Z**, **You Q**, **Zhang C**, **Yang L**, **Duan X**. The use of particulated juvenile allograft cartilage for the repair of porcine articular cartilage defects. *Am J Sports Med*. 2019;47(10):2308–2315.
33. **Farr J**, **Tabet SK**, **Margerrison E**, **Cole BJ**. Clinical, radiographic, and histological outcomes after cartilage repair with particulated juvenile articular cartilage: a 2-year prospective study. *Am J Sports Med*. 2014;42(6):1417–1425.
34. **You Q**, **Liu Z**, **Zhang J**, **et al**. Human amniotic mesenchymal stem cell sheets encapsulating cartilage particles facilitate repair of rabbit osteochondral defects. *Am J Sports Med*. 2020;48(3):599–611.
35. **Li Y**, **Liu Z**, **Jin Y**, **et al**. Differentiation of human amniotic mesenchymal stem cells into human anterior cruciate ligament fibroblast cells by in vitro coculture. *Biomed Res Int*. 2017;2017:7360354.
36. **Zhang J**, **Liu Z**, **Tang J**, **et al**. Fibroblast growth factor 2-induced human amniotic mesenchymal stem cells combined with autologous platelet rich plasma augmented tendon-to-bone healing. *J Orthop Translat*. 2020;24:155–165.
37. **Zhu X**, **Liu Z**, **Wu S**, **et al**. Enhanced tenogenic differentiation and tendon-like tissue formation by Scleraxis overexpression in human amniotic mesenchymal stem cells. *J Mol Histol*. 2020;51(3):209–220.
38. **Xiao P**, **Zhu Z**, **Du C**, **et al**. Silencing Smad7 potentiates BMP2-induced chondrogenic differentiation and inhibits endochondral ossification in human synovial-derived mesenchymal stromal cells. *Stem Cell Res Ther*. 2021;12(1):132.
39. **Brittberg M**, **Peterson L**. Introduction to an articular cartilage classification. *ICRS Newsletter*. 1998;1:5–8.
40. **Mainil-Varlet P**, **Van Damme B**, **Nesic D**, **Knutsen G**, **Kandel R**, **Roberts S**. A new histology scoring system for the assessment of the quality of human cartilage repair: ICRS II. *Am J Sports Med*. 2010;38(5):880–890.
41. **Shu J**, **He X**, **Li H**, **et al**. The beneficial effect of human amnion mesenchymal cells in inhibition of inflammation and induction of neuronal repair in EAE mice. *J Immunol Res*. 2018;2018:5083797.

42. **Sanluis-Verdes A**, **Yebra-Pimentel Vilar MT**, **García-Barreiro JJ**, **et al**. Production of an acellular matrix from amniotic membrane for the synthesis of a human skin equivalent. *Cell Tissue Bank*. 2015;16(3):411–423.
43. **Zhou H**, **Wang L**, **Zhang C**, **et al**. Feasibility of repairing full-thickness skin defects by iPSC-derived epithelial stem cells seeded on a human acellular amniotic membrane. *Stem Cell Res Ther*. 2019;10(1):155.
44. **Minjuan W**, **Jun X**, **Shiyun S**, **et al**. Hair follicle morphogenesis in the treatment of mouse full-thickness skin defects using composite human acellular amniotic membrane and adipose derived mesenchymal stem cells. *Stem Cells Int*. 2016;2016:8281235.
45. **Zhang Q**, **Xiang E**, **Rao W**, **et al**. Intra-articular injection of human umbilical cord mesenchymal stem cells ameliorates monosodium iodoacetate-induced osteoarthritis in rats by inhibiting cartilage degradation and inflammation. *Bone Joint Res*. 2021;10(3):226–236.
46. **Zong Z**, **Zhang X**, **Yang Z**, **et al**. Rejuvenated ageing mesenchymal stem cells by stepwise preconditioning ameliorates surgery-induced osteoarthritis in rabbits. *Bone Joint Res*. 2021;10(1):10–21.
47. **Sanghani-Kerai A**, **Black C**, **Cheng SO**, **et al**. Clinical outcomes following intra-articular injection of autologous adipose-derived mesenchymal stem cells for the treatment of osteoarthritis in dogs characterized by weight-bearing asymmetry. *Bone Joint Res*. 2021;10(10):650–658.
48. **Hefka Blahnova V**, **Dankova J**, **Rampichova M**, **Filova E**. Combinations of growth factors for human mesenchymal stem cell proliferation and osteogenic differentiation. *Bone Joint Res*. 2020;9(7):412–420.
49. **Chen C-Y**, **Liu S-H**, **Chen C-Y**, **Chen P-C**, **Chen C-P**. Human placenta-derived multipotent mesenchymal stromal cells involved in placental angiogenesis via the PDGF-BB and STAT3 pathways. *Biol Reprod*. 2015;93(4):1–25.
50. **Beeravolu N**, **McKee C**, **Alamri A**, **et al**. Isolation and characterization of mesenchymal stromal cells from human umbilical cord and fetal placenta. *J Vis Exp*. 2017;(122):55224.
51. **Schroeder DI**, **Blair JD**, **Lott P**, **et al**. The human placenta methylome. *Proc Natl Acad Sci U S A*. 2013;110(15):6037–6042.
52. **Silini AR**, **Cancelli S**, **Signoroni PB**, **Cargnoni A**, **Magatti M**, **Parolini O**. The dichotomy of placenta-derived cells in cancer growth. *Placenta*. 2017;59(2):154–162.
53. **Marmotti A**, **Bruzzone M**, **Bonasia DE**, **et al**. Autologous cartilage fragments in a composite scaffold for one stage osteochondral repair in a goat model. *Eur Cell Mater*. 2013;26:15–31; discussion 31-2.
54. **Benya PD**, **Shaffer JD**. Dedifferentiated chondrocytes reexpress the differentiated collagen phenotype when cultured in agarose gels. *Cell*. 1982;30(1):215–224.
55. **Matsubara N**, **Nakasa T**, **Ishikawa M**, **Tamura T**, **Adachi N**. Autologous meniscus fragments embedded in atelocollagen gel enhance meniscus repair in a rabbit model. *Bone Joint Res*. 2021;10(4):269–276.
56. **Adkisson HD**, **Gillis MP**, **Davis EC**, **Maloney W**, **Hruska KA**. In vitro generation of scaffold independent neocartilage. *Clin Orthop Relat Res*. 2001;(391 Suppl):S280–S294.
57. **Adkisson HD**, **Martin JA**, **Amendola RL**, **et al**. The potential of human allogeneic juvenile chondrocytes for restoration of articular cartilage. *Am J Sports Med*. 2010;38(7):1324–1333.
58. **Adkisson HD**, **Milliman C**, **Zhang X**, **Mauch K**, **Maziarz RT**, **Streeter PR**. Immune evasion by neocartilage-derived chondrocytes: Implications for biologic repair of joint articular cartilage. *Stem Cell Res*. 2010;4(1):57–68.
59. **Liu H**, **Zhao Z**, **Clarke RB**, **Gao J**, **Garrett IR**, **Margerrison EEC**. Enhanced tissue regeneration potential of juvenile articular cartilage. *Am J Sports Med*. 2013;41(11):2658–2667.
60. **Bianchi VJ**, **Lee A**, **Anderson J**, **et al**. Redifferentiated chondrocytes in fibrin gel for the repair of articular cartilage lesions. *Am J Sports Med*. 2019;47(10):2348–2359.

Author information:
- Z. Jun, PhD, Clinician
- W. Yuping, PhD, Clinician
- H. Yanran, PhD, Clinician
- W. Zhilin, PhD, Clinician
- L. Xiaoji, PhD, Professor
  Department of Orthopedics, The First Affiliated Hospital of Chongqing Medical University, Chongqing, China.
- L. Ziming, PhD, Clinician
- L. Yuwan, PhD, Clinician
  Peking University Third Hospital, Beijing, China; Zunyi Medical University, Zunyi, China.
- Z. Xizhong, PhD, Clinician, Department of Spine Surgery, The Third Affiliated Hospital of Sun Yat-sen University, Guangzhou, China.

Author contributions:
- Z. Jun: Investigation, Writing – original draft.
- W. Yuping: Investigation.
- H. Yanran: Investigation.
- L. Ziming: Formal analysis.
- L. Yuwan: Formal analysis.
- Z. Xizhong: Formal analysis.
- W. Zhilin: Formal analysis.
- L. Xiaoji: Conceptualization, Methodology, Resources.

Funding statement:
- The authors disclose receipt of the following financial or material support for the research, authorship, and/or publication of this article: the National Natural Science Foundation of China (NSFC) (nos. 8187090823).

ICMJE COI statement:
- The authors declare that they have no competing interests.

Data sharing:
- The datasets used and/or analyzed during the current study are available from the corresponding author on reasonable request.

Acknowledgements:
- We are grateful for the Department of Immunology, Zunyi Medical University, Guizhou, and all persons in this department. We thank You Qi, Yang Qifan, and Ge Zhen for their help of this work.

Ethical review statement:
- The study was reviewed and approved by the Ethics Committee of the Affiliated Hospital of Zunyi Medical University.

Open access funding
- The authors confirm that the open access fee for this study was self-funded.